Physiological implications of impaired de novo Coenzyme A Biosynthesis in Drosophila melanogaster

Bosveld, Floris

CHAPTER 4.

De novo CoA biosynthesis is required to maintain DNA integrity in a *Drosophila* model of Pantothenate Kinase-Associated Neurodegeneration

Floris Bosveld[1], Anil Rana[1], Petra E. van der Wouden[1], Willy Lemstra[1], Martha Ritsema[1], Harm H. Kampinga[1], Ody C. M. Sibon[1]

[1]Department of Cell Biology, Section of Radiation & Stress Cell Biology,
University Medical Centre Groningen, University of Groningen, Groningen, The Netherlands

Submitted for publication

ABSTRACT

From a forward genetic screen in *Drosophila*, aimed to identify genes involved in surviving induced DNA damage, we isolated *dPPCS* (the second enzyme of the CoA biosynthesis pathway) as a novel gene required to maintain DNA integrity. The complete *Drosophila* CoA synthesis route was dissected, annotated and additional mutants that carry mutations in CoA enzymes were obtained (*dPANK/fumble*) or generated (*dPPAT-DPCK*) and used for further investigation. *Drosophila* CoA mutants are hypersensitive to ionizing radiation, suffer from altered lipid homeostasis, and the larval brains display increased apoptosis and elevated levels of damaged DNA. In addition, disruption of CoA synthesis in general provokes neurodegeneration in adults. Our data provide the first comprehensive analysis of the physiological implications of mutations in the entire CoA biosynthesis route in an animal model system. Surprisingly, our findings reveal a major role of this conserved metabolic pathway in maintaining DNA and cellular integrity during development of the central nervous system, and the data explain how impairment of CoA synthesis during development can lead to neurodegeneration in *Drosophila*. In humans, mutations in the *PANK2* gene, coding for the first enzyme in the CoA biosynthesis pathway, are associated with Pantothenate Kinase-Associated Neurodegeneration (PKAN). Currently, the pathogenesis of this devastating neurodegenerative disorder is poorly understood. The presented *Drosophila* model will be of help to understand the consequences of impaired *de novo* CoA synthesis in higher eukaryotes and may provide insights in the pathogenesis of PKAN.

CONTENTS

INTRODUCTION

As the major acyl carrier in all organisms coenzyme A (CoA) constitutes an essential cofactor necessary to support cellular metabolism (reviewed in ref. 1). *De novo* CoA is synthesized from vitamin B_5 which is converted by the subsequent action of 5 enzymes: PANK, PPCS, PPCDC-PPAT and DPCK[2-5]. The consequences of impaired CoA synthesis in higher eukaryotes has not been investigated in detail. However, genetic analysis linked a neurological disorder to mutations in the human *PANK2* gene: pantothenate kinase-associated neurodegeneration or PKAN (OMIM 234200)[2], indicating that intact PANK2 function is required for neuronal function. PKAN is classically characterized by motor symptoms such as dystonia or parkinsonism, cognitive decline, and retinal degeneration, which are often presented during early childhood and these symptoms progress rapidly (reviewed in ref. 6). Patients with PKAN display iron accumulation in specific areas of the brain[6] and high levels of cysteine in the brains of patients that were clinically diagnosed with PKAN have been reported[7]. It was postulated that oxidative damage as a result of the Fenton reaction fuelled by high concentrations of Fe/cysteine[8] underlies PKAN disease pathogenesis[2]. Although the clinical symptoms and histological features of PKAN are extensively examined, it is still largely unknown how a deficiency in PANK2 affects neuronal survival and which cellular alterations are responsible for the onset and the progression of the disease[6,9,10].

In a forward genetic screen using *Drosophila*, aimed to identify novel genes involved in DNA damage responses, we identified *dPPCS* as a gene required to survive ionizing radiation (IR). We further employed *Drosophila* to study the effect of mutations in genes coding for CoA biosynthesis enzymes and *dPANK/fbl*[11], *dPPCS* and *dPPAT-DPCK* mutant phenotypes were analyzed in detail. We demonstrate that altered CoA biosynthesis in general causes hypersensitivity to IR, impaired DNA and cellular integrity during larval brain development. Moreover, mutations in genes coding for CoA biosynthesis enzymes induce neurodegeneration, reduce lifespan, affect lipid homeostasis and result in progressive neuronal dysfunction in adult flies. Interestingly, exposure to IR leads to impaired locomotor activity in young wild-types and locomotor activity is further impaired in CoA mutants by IR, indicating that IR hypersensitivity, DNA damage and neuronal dysfunction are linked in CoA mutant flies. We show that, although young mutant flies display decreased resistance to oxidative stress, oxidative damage is not the sole cause of neuronal dysfunction in young flies. The presented *Drosophila* model may be of help to understand how impaired CoA biosynthesis elicits a neurodegenerative phenotype in animals.

MATERIAL AND METHODS

***Drosophila* stocks and genetics:** Fly stocks were maintained at 22 °C according to standard protocols. For wild-type preparations y^1w^{1118} was used. The ROS overexpression line *ZnSod-Cat-Trx* was a gift from R. S. Sohal (Southern Methodist University, USA) and is previously described[12]. *Df(3R)Dl-KX23*, *dPANK/fbl*^{1} (*fbl*^{1}), eGFP balancer chromosomes and the *P[SUPor-P]*^{KG04801} lines were obtained from the Bloomington Stock Centre (Indiana University, USA). *dPPCS*^{33} and *dPPAT-DPCK*^{43} were generated by imprecise excision of *P[lacW]dPPCS*^{1} and *P[SUPor-P]*^{KG0480} respectively[13]. Imprecise excision in *dPPCS*^{33} resulted in a 1447 bp deletion, which removes the first intron of the *dPPCS* mRNA. In *dPPAT-DPCK*^{43} the transposon left behind a scar of ~350 bp P element specific DNA ~50 bp upstream of the *dPPAT-DPCK* gene (CG10575 at 64E7) (not shown). Homozygous *dPPAT-DPCK*^{43} are sensitive to IR and females are impaired fertile. When *dPPAT-DPCK*^{43} was placed over *Df(3L)ZN47* (64C;65C), transheterozygous flies were sensitive to IR and displayed fertility defects (not shown). These phenotypes were not caused by a contribution of the neighbouring gene (CG5505) since the mRNA expression levels (as determined by RT-PCR) of CG5505 did not show significant changes in *dPPAT-DPCK*^{43} mutant flies compared to wild-type

expression levels ($p < 0.4$, n=3), while the expression of CG10575 was reduced in *dPPAT-DPCK*$^{43/43}$ males ($p < 0.03$, n=3) (not shown), demonstrating that the *dPPAT-DPCK*^{43} allele is a hypomorphic allele of the *dPPAT-DPCK* gene.

Sensitivity screening and *dPPCS* mapping: *dPPCS*^{1} was created by transposon mediated mutagenesis[14] and the insertion site was determined after plasmid rescue analysis[15]. PCR mapping combined with complementation tests by means of standard crosses to deficient chromosomes encompassing the identified polythene regions confirmed the localisation of the P element (not shown). Heterozygous flies were crossed (day 1-3) in standard food vials and on day 5 larvae were exposed to 20 Gy of γ-rays delivered by a Cs^{137} unit (type IBL 637, CIS Biointernational) or left untreated. At day 14-21 the percentage of homozygous adults in the F1 generation was determined. In a similar screen larvae were fed a 0.5 ml 100 mM L-cysteine (Sigma) solution in water or water only. At least three independent experiments were performed.

Molecular techniques: For the construction of *P[dPPCS]* transgenic flies the *dPPCS* cDNA was PCR amplified with primers 5'-GAACTCCTACGCTCAGAAC-3' and 5'-GATGCCACGCCATTGAT-3' from EST clone GH03502/UG11G5 (Children's Hospital Oakland Research Institute, USA). The fragment was *Cla*I/*Eco*RI subcloned into pBUF, provided by J. Sekelsky (University of Carolina, USA), behind the ubiquitin promoter and in frame with a NH_2-terminal FLAG epitope. Next, the promoter-FLAG-cDNA was cloned between the *Kpn*I and *Eco*RI sites in front of a Bgh polyadenylation signal present in pCaSpeR4-Pme1-Bgh provided by L. G. Fradkin (Leiden University Medical Centre, The Netherlands) to yield pCasper4-Pme1-ubiquitin-FLAG-dPPCS-Bgh. Transgenic flies were created by Genetic Services Inc. (Sudbury, USA). To clone the 5'-UTR of the *dPPCS* mRNA total RNA was extracted from *dPPCS*$^{1/1}$ and control adult males using TRIreagent (Sigma), and polyadenylated RNA was purified with Oligotex mRNA kit (Qiagen). The BD SMART™ RACE cDNA Amplification Kit (BD Biosciences Clontech) and the *dPPCS* specific primer 5'- GGCGGCAGGTGCGTGTTGTAGAAGT-3' were used to amplify the 5'-UTR. After nested PCR with the *dPPCS* specific primer 5'-CTGCTAATTGGCCGACAAACGGAAG-3' the resulting fragments were TA cloned into pCR2.1 (Invitrogen) and sequenced. Polyclonal antibodies were raised in rabbits against synthetic peptides of dPANK/Fbl (YFEPKDITPDEQDREC and CDEPPEKAPTSKHSTR) and dPPCS (CDMMPTHKMQSGDGAP and CVQKHGEFISNAQQRQ) and affinity purified (Eurogentec).

Immunoblot analysis: Larval brains, adult testis and ovaries were dissected in PBS. Flies were maintained in cages on apple juice plates containing yeast paste to collect embryos. Samples were lysed in RIPA buffer supplemented with proteinase inhibitor cocktail 1697498 (Roche), sonicated and the protein content determined using the Bio-Rad DC protein assay kit (Bio-Rad). Protein extracts were separated on 12.5% SDS-PAGE gels, transferred to nitrocellulose membranes (BioRad Mini-Protean electrophoresis system), blocked in PBS + 0.1% Tween20 (PBST) supplemented with 5% non-fat milk and the membranes were incubated with anti-dPANK (1:4000) or anti-dPPCS (1:1500) antibodies in PBST + 5% non-fat milk. After incubation blots were washed with PBST and incubated with HRP-conjugated goat anti-rabbit IgG (Amersham) secondary antibodies (1:2000). The antibody complexes were visualized using an enhanced chemiluminescent (ECL) kit (Amersham). After 1 day the same blots were incubated with mouse anti-γ-tubulin (1:5000, Sigma) or mouse anti-β-actin (1:5000, Abcam) antibodies diluted in PBST. After incubation blots were processed as described. To determine the relative dPPCS protein levels in *dPPCS* mutant and wild-type larval brains, Western blots from 4 independent experiments were quantified with ImageJ (http://rsb.info.nih.gov/ij/) using β-actin or γ-tubulin as internal references. The area x mean intensity of the reference was divided by the area x mean intensity of dPPCS and normalized to wild-type ratios.

Lipid analysis: For the triglyceride assay, 10 5-day-old (wild-type and *dPANK/fbl*$^{1/1}$) or 14-day-old (wild-type, dPPCS, *dPPAT-DPCK*^{43}) males were grinned in 100 µl PBS. Triglycerides were measured using the Stanbio LiquiColor assay kit, according to the manufacturer's instructions. The protein concentration of the same homogenates was determined with the Bio-Rad DC protein assay kit. Mutant triglyceride levels were normalized to percentages of wild-type levels and represent the average of 3 independent experiments. To determine the amount of phospholipids approximately 20 mg of fly heads from a mixture of 14-day-old female and male adults was homogenized and the protein content determined with the Bio-Rad DC protein assay. Lipids were extracted, separated and quantified essentially as described in ref. 16.

Immunohistochemistry: Mutant alleles were maintained over an eGFP expressing TM3 balancer and homozygous third instar wandering larvae were identified by the absence of eGFP expression. Larval brains were dissected in PBS, fixed in PBS + 4% formaldehyde, washed with PBS + 0.3% Triton X-100 (PBT), blocked in PBT + 5% bovine serum albumin (BSA) and incubated with primary antibodies in blocking buffer. After incubation, brains were washed with blocking buffer and incubated with secondary antibodies in blocking buffer. Primary antibodies used included mouse anti-Histone H3 pS10 (1:100, Cell Signaling) and rabbit anti-Histone H2AvD pS137 (1:100, Rockland). Secondary antibodies included FITC-conjugated goat anti-mouse IgG (1:200, Jackson ImmunoResearch) and Cy3-conjugated goat anti-rabbit IgG (1:200, Jackson ImmunoResearch). After immunolabeling brains were washed,

mounted in citifluor (Agar Scientific) and analyzed by fluorescent microscopy (FM) or confocal laser scanning microscopy (CLSM). CLSM images represent maximal projections of a z-stack (0.5-1 μm/scan) and were obtained with a 63X/1.32 oil lens (Leica TCS SP2 DM RXE). Acridine orange staining was performed by dissecting larval brains in Schneider's *Drosophila* medium (S2) without serum (Invitrogen). After dissection brains were incubated for 4 m in S2 medium containing 1.6 μM acridine orange, washed with PBS for 30 s, mounted and immediately investigated by FM (Leica CTR6000). Brains were classified either as enhanced apoptotic or normal. Irradiation of larvae used to inspect mitotic abnormalities was performed in Petri dishes. After exposure to 20 Gy of γ-rays a few drops of water were added to the dishes and larvae were allowed to recover for 5 h before dissection. pH3Ser10 labeled chromatin was analyzed using a 100x magnification (100x/1.3 oil immersion objective) with 1.5x optivar on an inverted FM (Olympus IMT-2). Mitotic figures were scored per focal plane and the percentage aberrant mitosis was calculated from the SUM of 7-11 focal planes scored per brain. The mitotic index (MI) of mutant brains was similar to the MI of wild-type brains (not shown). The total amount of γ-H2AvD positive cells was counted in entire brains. Captured images were processed using Leica Software and Paint Shop Pro. For histological examination of brain/retina/pericerebral fat body morphology, heads from 30-d-old flies were fixed in 4% formaldehyde and embedded in epon. 1 μm horizontal sections were stained with 1% toluidine blue and 1% borax and investigated with an Olympus BX50 light microscope (Olympus).

Physiological assays: Adult performance assays were carried out with male flies. Flight and geotaxis were measured on day 7 (young) and day 14 (aged). *dPANK/fbl*$^{1/1}$ flies were only assayed on day 5. Wing abnormalities were determined in aged flies (*dPANK/fbl*$^{1/1}$ on day 5). 3 h prior to the assays flies were anesthetized with CO_2, investigated for visible wing damage and discarded. Flies were first used for the climbing assay and subsequently for the flight assay. Flight was assayed by pouring 10-20 flies in a glass graduated cylinder (1000 ml) coated with paraffin oil and scoring their collision height[17]. The average performance coefficient was determined by scoring the landing height of the best performing group in each trail, where a group is defined as the % of flies that landed at: 10 (1000-900 ml), 9 (900-800 ml), 8 (800-700 ml), 7 (700-600 ml), 6 (600-500 ml), 5 (500-400 ml), 4 (400-300 ml), 3 (300-200 ml), 2 (200-100 ml), 1 (100-0 ml). At least 200 flies were used in the flight assay (for *dPANK/fbl*$^{1/1}$ at least 100 flies were used). In the climbing assay (geotaxis), 10 flies were tested for their ability to climb upside a 250 ml glass cylinder. The time required for 50% of the flies to cross the 150 ml line was reordered[18]. 10 cohorts of flies were tested and the performance over 5 trails for each cohort was averaged. The absolute climbing ability was determined by tapping 10-20 flies to the bottom of a standard food vial and counting the flies that were attached to the side after 30 s. 10 trails were performed for each cohort and the average climbing ability was calculated from at least 7 cohorts. To determine the effect of IR on adult performance the absolute ability to climb was analyzed 24 h AE. The % of untreated flies that was able to climb was compared with the % of flies that was able to climb after exposure to 20 Gy. 10 cohorts of untreated and irradiated flies were analyzed. Irradiation was performed as described for sensitivity screening. Longevity was measured for both females and males and both sexes were present in about equal proportions in all groups. Flies were kept at 10-20/vial and every 2-4 days flies were transferred to fresh vials and the death flies were scored. ROS sensitivity was measured by placing 15-25 24-h-old male flies, after 6 h starvation, in vials containing filter paper soaked with H_2O or soaked in H_2O containing 5% glucose and 100 mM DTT (Sigma), 5% H_2O_2 or 20 mM paraquat (Sigma). Twice a day death flies were scored.

Statistical analysis: *P*-values were calculated using the Student's *t*-test (two-tailed and where appropriate with equal or unequal variance). Survival curves were analyzed by the method of Kaplan and Meier using SigmaStat 3.5. *P*-values < 0.05 were considered significant.

RESULTS

Mutations in the phosphopantothenoylcysteine synthetase locus induce hypersensitivity to genotoxic stress

In a forward genetic screen using P element insertion lines, aimed to identify novel genes involved in DNA damage responses in flies, we identified a mutant hypersensitive to IR (**Fig. 1A**). When larvae were exposed to IR the survival of homozygous adults decreased, implying loss of function of a gene essential to survive DNA damage. In the mutant, the P element was mapped within the 5'-UTR of an uncharacterized gene CG5629 (**Fig. 1B**) that encodes two mRNAs only differing in their 3'-UTR and that both encode an ORF of 313 amino acids. *In silico* analyses revealed that CG5629 encodes a structural ortholog of the human

phosphopantothenoylcysteine synthetase (PPCS), which constitutes the second enzyme in the biosynthesis of CoA (**Supplementary Figs. S1-S2, Table S1**). Therefore, the mutant will be referred to as *d(Drosophila)PPCS*^{1}. Using rapid amplification of cDNA ends (RACE), we cloned the 5'-UTR of CG5629 in *dPPCS*^{1} mutants and found it to be truncated by approximately 250 bp

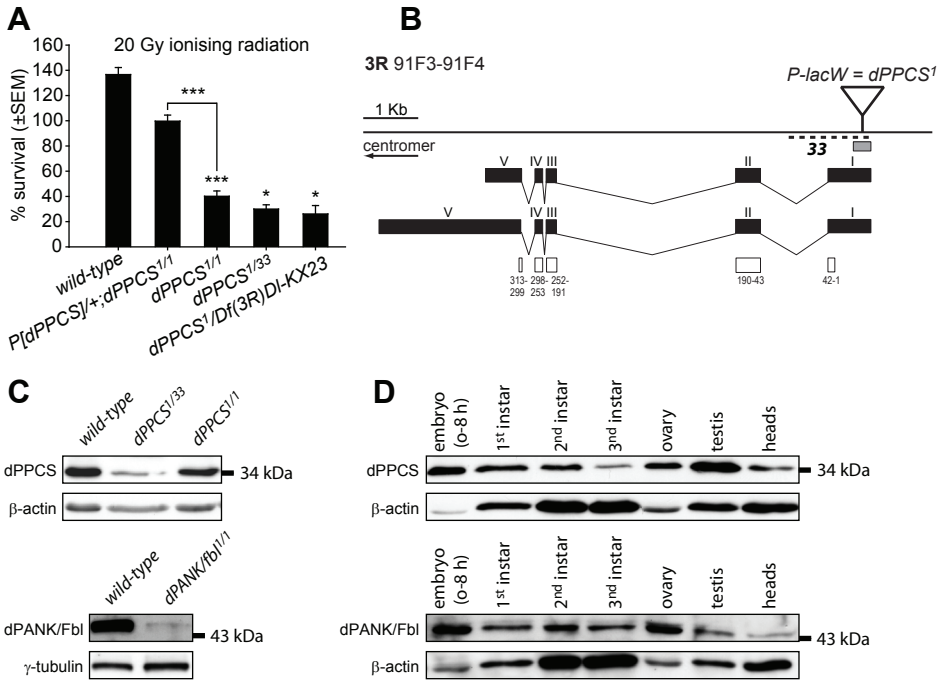

Figure 1. Mutations in phosphopantothenoylcysteine synthetase sensitizes *Drosophila* to IR.
(A) IR survival graph. The percentage of homozygous survivors was calculated under control conditions and after exposure of larvae to 20 Gy IR. The percentage homozygous survivors under control conditions was set to 100%. Survival of *dPPCS*^{1} mutants is reduced after 20 Gy. *dPPCS*^{1} placed over a deficiency chromosome (*Df(3R)Dl-KX23*, 91C7-D03;92A5-08) or over a KO allele (*dPPCS*^{33}) also displayed hypersensitivity to IR. Ectopic overexpression of a FLAG-tagged dPPCS cDNA (*P[dPPCS]*) under control of an ubiquitin promotor suppressed the hypersensitivity of the *dPPCS*^{1} allele to IR. (*$p < 0.05$, ***$p < 0.001$ as determined by *t*-test).
(B) Physical map of the *D. melanogaster* phosphopantothenoylcysteine synthetase (*dPPCS*) locus. The region depicted comprises cytological position 91F3-91F4 of chromosome 3R and harbors the CG5629 gene. CG5629 encodes two mRNAs as evident from the EST database (www.fruitfly.org). Both transcripts have 5 exons and encrypt a 313 amino acid ORF that represent the tentative fly PPCS ortholog (**Supplementary Fig. S1-S2**). The P-lacW insertion allele *dPPCS*^{1} is indicated by the triangle. Transcripts are indicated by black boxes and their encoded proteins are depicted underneath (white boxes, numbers correspond to amino acid positions). 5'-RACE of mRNA isolated from *dPPCS*$^{1/1}$ flies revealed a ~250 bp truncation of the *dPPCS* mRNA (graybox). Removal of the first exon (1447 bp deletion) from CG5929 (*dPPCS*^{33}, dashed line) induces lethality during the first instar larval stadium.
(C) Western blot analyses of wild-type, *dPPCS*$^{1/1}$, *dPPCS*$^{1/33}$, and *dPANK/fbl*$^{1/1}$ third instar larval brain extracts by using polyclonal antibodies raised against dPPCS (upper panel) and dPANK/Fbl (lower panel). dPPCS protein expression is reduced in brains from *dPPCS*$^{1/1}$ mutants (a 13% reduction (± 4 SEM, n=4)) and reduced in brains from *dPPCS*$^{1/33}$ mutants (a 28% reduction (± 9 SEM, n=4)) compared to wild-types. dPANK expression is severely reduced in *dPANK/fbl*$^{1/1}$ brains. Blots were incubated with antibodies against β-actin or γ-tubulin as loading controls.
(D) Western blot showing that the dPPCS (upper panel) and dPANK (lower panel) proteins are expressed during development and in all tissues tested.

(**Fig. 1B**). Hypersensitivity to IR was also observed when *dPPCS*^{l} was placed over *Df(3R)Dl-KX23*, covering at least 50 genes surrounding the *dPPCS* locus (**Fig. 1A**). Ectopic expression of a FLAG-tagged dPPCS cDNA (*P[dPPCS]*) under control of an ubiquitin promotor in the *dPPCS*$^{l/l}$ background (*P[dPPCS]/+;dPPCS*$^{l/l}$) rescued the hypersensitivity to IR (**Fig. 1A**). This transgene (partly) suppressed all the phenotypes discussed in this manuscript, proving that they were due to a mutation in the *dPPCS* locus. A null mutation (*dPPCS*^{33}) was generated by imprecise P element excision[13] (**Fig. 1B**) and in contrast with *dPPCS*$^{l/l}$ flies, *dPPCS*$^{33/33}$ mutants die as first instar larvae. However, *dPPCS*$^{l/33}$ mutants were viable, hypersensitive to IR and these transheterozygous mutants frequently had a more severe phenotype as compared to *dPPCS*$^{l/l}$ mutants. Together these results demonstrate that *dPPCS*^{l} constitutes a hypomorph and viable allele of the *dPPCS* gene, while *dPPCS*^{33} is a null and lethal allele, and imply that *dPPCS* is essential in *Drosophila*. Intriguingly, mutations in *dPPCS* induce IR hypersensitivity, indicating a link between CoA biosynthesis and DNA integrity.

The *de novo* CoA synthesis pathway is conserved in *Drosophila*

De novo synthesis of CoA occurs in a conserved metabolic route in which vitamin B_5 is subsequently modified by the action of 5 enzymes: PANK, PPCS, PPCDC, PPAT and DPCK (**Fig. 2A**)[4,5,19,20]. Unlike in other model organisms, *de novo* CoA biosynthesis in *Drosophila* is largely unknown. We employed *in silico* analyses and found 5 *Drosophila* loci coding for orthologs of PANK (*dPANK/fbl*), PPCS (*dPPCS*), PPCDC (*dPPCDC*), a bifunctional PPAT-DPCK (*dPPAT-DPCK*), and a single DPCK (*dDPCK*) (**Fig. 2B**, see **Supplementary Fig. S1-2**).

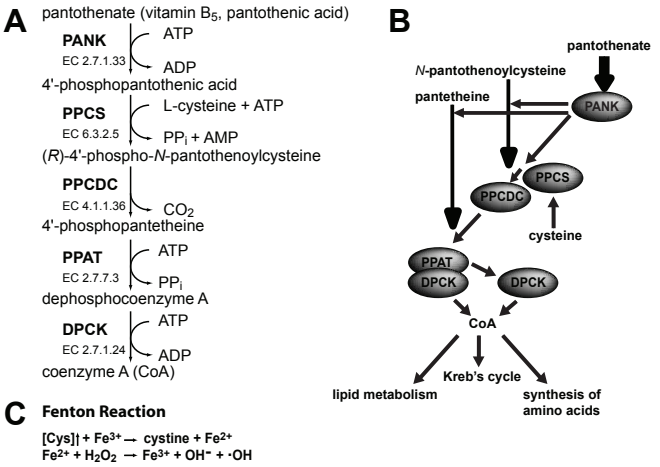

Figure 2. CoA biosynthesis in *Drosophila*.
(A) Universal pathway leading to *de novo* CoA synthesis. Higher eukaryotes depend on dietary pantothenate to produce CoA[21,24,25,27]. Pantothenate is phosphorylated to 4'-phosphopantothenate by pantothenate kinase (PANK). Next a cysteine is added by the 4'-phosphopantothenoylcysteine synthetase (PPCS) to form (*R*)-4'-phospho-*N*-pantothenoylcysteine which is decarboxylated by (*R*)-4'-phospho-*N*-pantothenoylcysteine decarboxylase (PPCDC) and produces 4'-phosphopantetheine. This 4'-phosphopantetheine receives an adenylyl group transferred from ATP mediated by 4'-phosphopantetheine adenylyltransferase (PPAT) and releases dephospho-CoA, which is then phosphorylated by dephospho-CoA kinase (DPCK) to finally yield CoA[2,4,5,19]. E.C. numbers are indicated.
(B) Schematic diagram of the *de novo* CoA biosynthesis in animals. The *Drosophila* genome encodes a single copy of *PANK*, *PPCS*, *PPCDC*, a bifunctional *PPAT-DPCK* and a *DPCK* (see **Supplementary Figs. S2-S1**). Mammalian PANK can also utilize pantetheine and *N*-pantothenoylcysteine to produce 4'-phosphopantetheine and (*R*)-4'-phospho-*N*-pantothenoylcysteine, respectively[28]. CoA and its acyl esters are utilized by many enzymes involved in the cellular metabolism including the Kreb's cycle, fatty acid production and the synthesis of some amino acids.
(C) Schematic view of the Fenton reaction. High intracellular cysteine can drive the Fenton reaction in the presence of iron, which results in the production of ROS[8].

The *Drosophila PANK* (*fumble* or *fbl*, further referred to as *dPANK/fbl*) gene was identified before as a gene required for normal mitosis and male fertility[11]. Mammals possess 4 *PANK* genes (*PANK1-4*), while flies only have 1 gene which is most identical to *PANK2*. In humans PANK2 is localized at mitochondria[21-23]. The *dPANK* locus encodes, in constrast to the human *PANK* genes, multiple isoforms and the dPANK protein partly co-localizes with mitochondria (A.R. and O.C.M.S., unpublished data). Thus in humans and *Drosophila* mitochondrial CoA synthesis may represent a crucial CoA production site[24-26].

To further analyze the *Drosophila* CoA enzymes, antibodies were raised against dPPCS and dPANK/Fbl. The expression levels of dPPCS and dPANK/Fbl (**Fig. 1C**) are affected in *dPPCS* and *dPANK/fbl* mutants respectively and consistent with their essential role in cellular metabolism in dPANK/Fbl and dPPCS are expressed during development and in all wild-type tissues investigated (**Fig. 1D**).

Mutations in genes required for *de novo* CoA biosynthesis cause neuronal dysfunction

During the analysis of the irradiation hypersensitive phenotype of *dPPCS* it was noticed that the mutant flies behaved in an uncoordinated manner. Previously, it was mentioned that *dPANK/fbl* flies also show movement abnormalities[11], however this was never demonstrated or further investigated. Moreover, PKAN is characterized by locomotor symptoms and thus impaired CoA biosynthesis is linked to behavior abnormalities in humans. The availability of a *dPANK/fbl* mutant[11] and a *dPPCS* mutant allowed us to examine whether and how impaired CoA biosynthesis gives rise to behavior abnormalities and whether this is due to neurodegeneration. In addition, we created an allelic series of the *dPPAT-DPCK* gene by mobilizing the *P[SUPor-P]^{KG04801}* insertion, which is located ~50 bp upstream of *dPPAT-DPCK* (www.flybase.org), and recovered a hypomorphic allele, *dPPAT-DPCK^{43}* (see methods). First we tested the CoA mutants for locomotor defects, an indicator of neuronal dysfunction[18]. To assess locomotor behavior, we evaluated the ability to climb and fly in young (7-d-old) and aged (14-d-old) flies. As can be seen in **Fig. 3A** the CoA mutants suffered from loss of locomotor function and locomotor dysfunction worsened in time (**Fig. 3B**). Progressive loss of locomotor activity could not be monitored

→ Figure 3. Mutations in CoA biosynthesis enzymes cause neuronal dysfunction.
(A-B) Different parameters of locomotor function in young (A, 7-d-old) and aged (B, 14-d-old) wild-type and mutant adults. Only 5-d-old *dPANK/fbl$^{1/1}$* males were assayed.
(A) The ability to initiate flight is reduced in young *dPANK/fbl*, *dPPCS* and *dPPAT-DPCK* mutant flies, reduced flight performance was only observed in *dPANK/fbl$^{1/1}$* flies and the ability to climb against gravity was impaired in all young CoA mutants compared to wild-types. Asterisks mark significant chances compared to wild-type flies.
(B) Wild-type flies showed no age-related decrease in flight behavior, but the ability to climb against gravity was significantly changed. Aged *dPPAT-DPCK* mutants showed no differences in the initiation of flight compared to young flies, but flight performance and the ability to climb against gravity were affected compared to young adults. Aged *dPPCS* mutants showed a decrease in flight behavior, but no decrease in geotaxis was found compared to young flies. Double rowed asterisks mark significant chances compared to young flies. (*$p < 0.05$, **$p < 0.005$, ***$p < 0.001$ as determined by *t*-test)
(C) Wing phenotypes in wild-type (Ca,b) and mutant flies (Cc,d). *dPANK/fbl*, *dPPCS* and *dPPAT-DPCK* mutant flies have held-out (Cc) and held-up (Cd) wings, quantified in (Ce), which are indicative of abnormal indirect flight muscle contraction. Number of flies investigated was; wild-type n=248, *dPANK$^{1/1}$* n=54, *dPPCS$^{1/1}$* n=269, *dPPCS$^{1/33}$* n=202, *dPPAT-DPCK$^{43/43}$* n=131.
(D) Lifespan curves of wild-type and mutant flies. Median survival of: wild-type (50 days, n=1045), *dPANK/fbl$^{1/1}$* (8 days, n=240), *dPPCS$^{1/1}$* (42 days, n=1230), *dPPAT-DPCK$^{43/43}$* (32 days, n=1043), *P[dPPCS]/+;dPPCS$^{1/1}$* (61 days, n=614). Lifespan curves of *dPANK/fbl$^{1/1}$*, *dPPCS$^{1/1}$* and *dPPAT-DPCK$^{43/43}$* significantly differ from the wild-type (log-rank, $p < 0.001$). The *P[dPPCS]* transgene restores *dPPCS$^{1/1}$* lifespan (log-rank, $p < 0.001$).

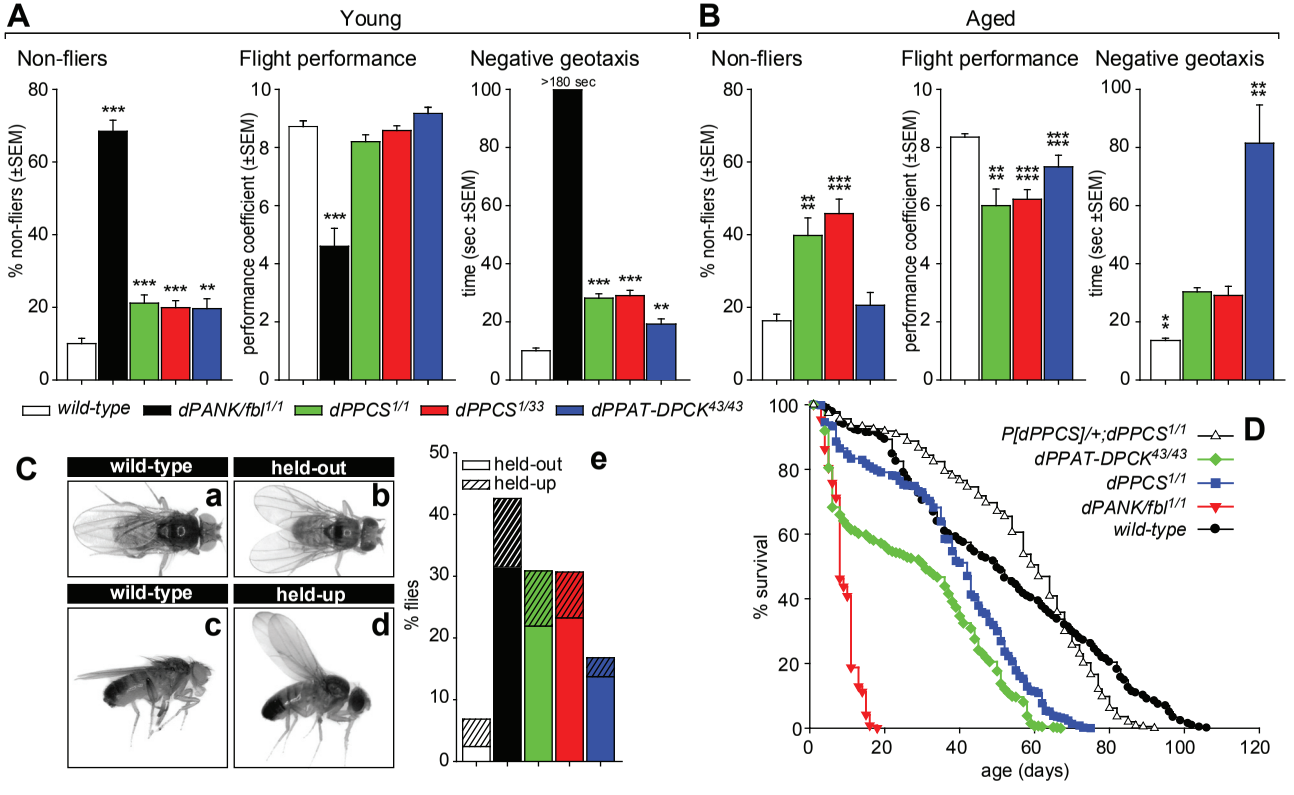
A
Young
Non-fliers
Flight performance
Negative geotaxis
% non-fliers (±SEM)
performance coefficient (±SEM)
time (sec ±SEM)
>180 sec
B
Aged
wild-type
dPANK/fbl1/1
dPPCS1/1
dPPCS1/33
dPPAT-DPCK43/43
C
wild-type
held-out
wild-type
held-up
a
b
c
d
e
held-out
held-up
% flies
D
P[dPPCS]/+;dPPCS1/1
dPPAT-DPCK43/43
dPPCS1/1
dPANK/fbl1/1
wild-type
% survival
age (days)

in *dPANK/fbl* mutants as they were extremely short-lived (see below). Consistent with their poor flight performance, *dPANK/fbl*, *dPPCS* and *dPPAT-DPCK* mutant flies had held-up and held-out wings, indicative of abnormal indirect flight muscle contraction (**Fig. 3C**). In addition to adult locomotor defects, *dPPCS* and *dPPAT-DPCK* mutant adults become paralytic when exposed to heat and *dPANK/fbl* and *dPPAT-DPCK* mutant larvae displayed locomotor defects (**Supplementary Figs. S3A-B**), features also associated with impaired function of the CNS.

Neurologically impaired flies often display reduced lifespan[18] and we also investigated longevity in the CoA mutants. Median survival of wild-type flies was 50 days. This was reduced to 8 days for *dPANK/fbl*$^{1/1}$ flies, 42 days for *dPPCS*$^{1/1}$ flies, and 32 days for *dPPAT-DPCK* mutant flies (**Fig. 3D**). Finally, to conclusively link altered CoA metabolism to neuronal dysfunction and neurodegeneration we analyzed the brains from 30-d-old wild-type and *dPPCS*$^{1/33}$ flies (**Fig. 4A-D**). The brains from *dPPCS*$^{1/33}$ displayed vacuolization, indicative for neurodegeneration (**Fig. 4B**). In addition, , *dPPCS*$^{1/33}$ flies suffered from retinal degradation as visible by the formation of vacuoles and loss of retinal structure (**Fig. 4D**).

In summary, although the severity of the phenotypes varies amongst the CoA mutants (**Supplementary Table S2**), our genetic analysis proves that disrupted CoA biosynthesis in general, underlies neuronal dysfunction.

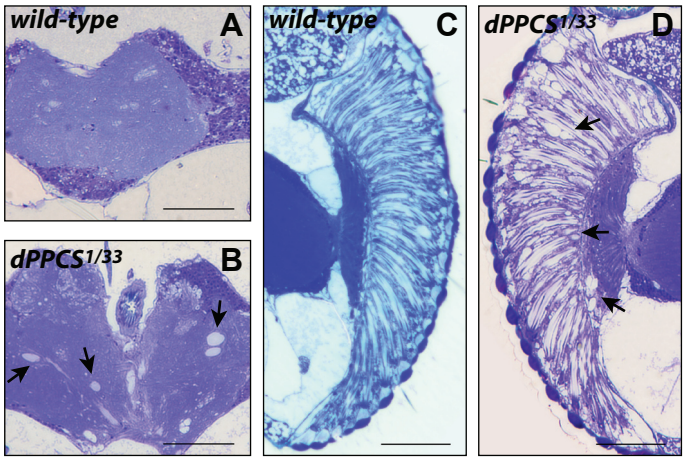

Figure 4. Neurodegeneration in *dPPCS* mutant brains.
(A-D) Horizontal head sections of 30-d-old wild-type **(A,C)** and *dPPCS*$^{1/33}$ mutants **(B,D)** stained with toludine blue. (B) *dPPCS*$^{1/33}$ brains display neurodegeneration visible by the formation of vacuoles (arrows). (D) *dPPCS*$^{1/33}$ flies display degeneration of photoreceptor cells visible by loss of retinal structure and formation of vacuoles (arrows).
Scale bars: 50 μm

CoA mutants are hypersensitive to ROS, but overexpression of SOD, CAT and TRX does not rescue neuronal dysfunction in young flies

Neurodegenerative diseases such as neurodegeneration with iron accumulation (NBIA), which includes PKAN, are classified as disorders associated with mitochondrial dysfunction (reviewed in ref. 29), and mitochondrial dysfunction associated with PANK deficiency has been reported in humans[21,24] and mice[25]. Because mitochondrial dysfunction can lead to decreased resistance to reactive oxygen species (ROS), increased oxidative stress may be one of the factors that induce neurodegeneration in organisms with impaired biosynthesis of CoA. In the biosynthesis pathway of CoA, cysteine incorporation occurs in a step downstream of PANK2 and it has also been postulated that PKAN disease pathogenesis is due to enhanced oxidative damage as a result of impaired Fe/cysteine metabolism which could drive the Fenton reaction (**Fig. 2C**) leading to the production of ROS[2].

Neurodegeneration in *Drosophila* is also frequently associated with increased oxidative stress (reviewed in ref. 30,31). To investigate whether oxidative stress contributes to the neurological phenotype of CoA mutant flies, we analyzed whether young (2-d-old) CoA mutant flies were sensitive to exogenously added ROS. Hereto, wild-types and mutants were exposed to paraquat, dithiothreitol (DTT) and H_2O_2. Mean survival of all CoA mutants was severely reduced after exposure to at least 2 of these ROS inducing agents (**Fig. 5A**). Overexpression of ROS scavengers (CuZn-superoxide dismutase (SOD), catalase (CAT), thioredoxin reductase (TRX)) (ref. 12 and references herein) in the *dPPCS*$^{1/1}$ mutant background (further referred to *SOD-CAT-TRX;dPPCS*$^{1/1}$ flies) suppressed the sensitivity to DTT and H_2O_2, and these *SOD-CAT-TRX;dPPCS*$^{1/1}$ flies were more resistant to paraquat than *dPPCS*$^{1/1}$ flies, proving that the ROS scavengers protected against increased oxidative stress induced by DTT, H_2O_2 and paraquat. Together these data demonstrate that CoA mutants are sensitive to ROS and suggest that CoA mutants suffer from higher levels of oxidative stress compared to wild-types.

Cysteine is incorporated in the second step of the *de novo* CoA biosynthesis pathway by PPCS (**Figs. 2A-B**). Therefore the prediction is that impaired function of *dPANK/fbl* or *dPPCS,* but not *dPPAT-DCPK* can lead to an accumulation of cysteine. In turn elevated levels of cysteine could drive the Fenton reaction (**Fig. 2C**) leading to the production of ROS[2]. If correct this will result in hypersensitivity to cysteine for *dPANK/fbl* and *dPPCS* mutants, but not for *dPPAT-DPCK* mutants. Consistent with this hypothesis survival of *dPANK/fbl* and *dPPCS* mutants, but not *dPPAT-DPCK*, decreased when larvae were fed with a 100 mM L-cysteine solution (**Fig. 5B**). This cysteine induced lethality was likely due to elevated oxidative damage, because survival of *SOD-CAT-TRX;dPANK/fbl*$^{1/1}$ and *SOD-CAT-TRX;dPPCS*$^{1/1}$ mutants was restored to wild-type levels in the presence of L-cysteine (**Fig. 5B**). Thus a Fenton reaction that generates ROS may exist in *dPANK/fbl* and *dPPCS* mutants. To investigate whether the observed decreased resistance to ROS contributes to neuronal dysfunction in young (7-d-old) flies we tested whether the ROS scavengers could rescue the locomotor defects associated with a mutation in *dPPCS*, *dPANK/fbl* or in *dPPAT-DPCK*. As can be seen in **Fig. 5C**, negative geotaxis was still compromised in *SOD-CAT-TRX;dPPCS*$^{1/1}$ and *SOD-CAT-TRX;dPPAT-DPCK*$^{43/43}$ flies (although not quantified with large numbers, visible inspection revealed that climbing of *SOD-CAT-TRX;dPANK/fbl*$^{1/1}$ flies was also not improved compared to *dPANK/fbl*$^{1/1}$). As a positive control, the *dPPCS* transgene (*P[dPPCS]/+;dPPCS*$^{1/1}$) showed normal wild-type performance. Although we can not exclude that oxidative damage contributes to the progressive loss of locomotor activity in aged (>14-d-old) flies, our data indicate that reduction of ROS levels by overexpressing SOD, CAT and TRX does not improve locomotor function in young flies. And although SOD, CAT and TRX may not be effective in scavenging ROS in every cellular compartment, these data point to additional causes other than oxidative damage that contribute to the onset of neuronal dysfunction in young CoA mutant flies.

Lipid biosynthesis is disrupted in *Drosophila* CoA mutants

CoA is an essential cofactor for the synthesis of many lipids[1] and impaired lipid metabolism has been implicated in PKAN disease pathogenesis[2,32,33]. In addition, mutations in lipid metabolism can cause neurodegeneration in flies[16,34,35], therefore it was investigated whether lipid homeostasis was disrupted in CoA mutant flies. In agreement with a role for *de novo* CoA synthesis in lipid homeostasis, the stored fatty acids in the form of triglycerides were reduced with ~25% in CoA mutant flies compared to wild-types (**Fig. 6A**). Similarly, the synthesis of

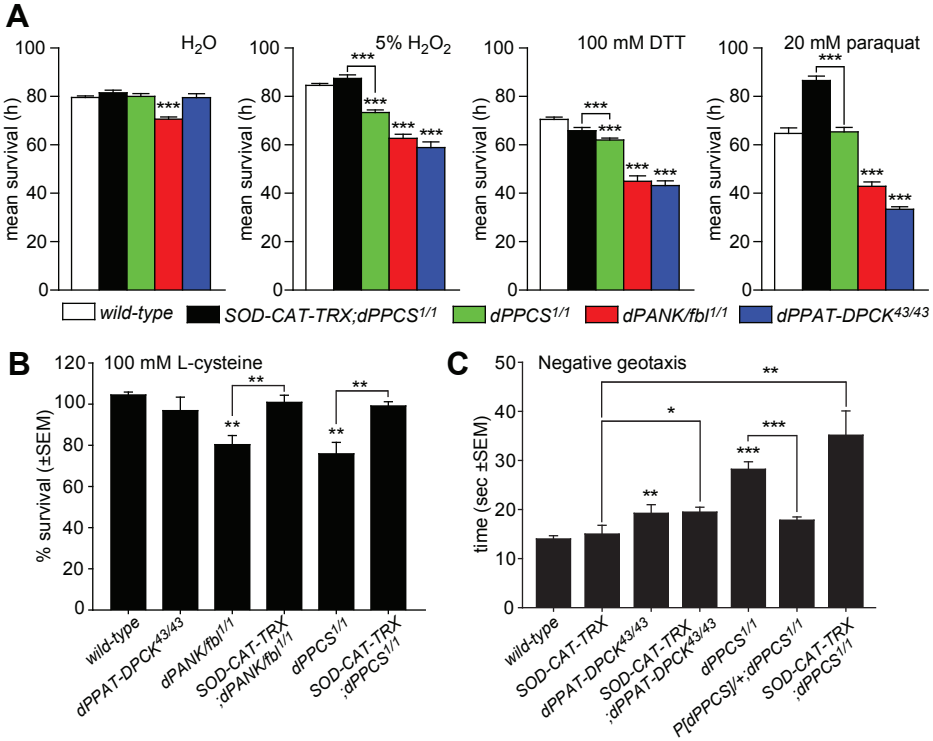

Figure 5. Oxidative damage is not the primary cause of neuronal dysfunction in CoA mutant flies.
(A) 2-d-old CoA mutant males were exposed to H_2O (control) and to ROS inducing agents (H_2O_2, DTT and paraquat dissolved in H_2O containing 5% glucose) and their survival was analyzed (mean survival ± standard error is depicted, log-rank ***$p < 0.001$). *dPANK/fbl*$^{1/1}$ mutants display sensitivity to wet starvation (H_2O). *dPANK/fbl*$^{1/1}$ and *dPPAT-DPCK*$^{43/43}$ flies are extremely sensitive to H_2O_2, DTT and paraquat, while *dPPCS*$^{1/1}$ flies show a decrease in resistance to H_2O_2 and DTT. Overexpression of ROS scavengers (CuZn-superoxide dismutase (SOD), a catalase (CAT) and a thioredoxin reductase (TRX)[12] in *dPPCS*$^{1/1}$ (*SOD-CAT-TRX;dPPCS*$^{1/1}$) suppressed the *dPPCS*$^{1/1}$ associated sensitivity to H_2O_2 and DTT, and increased the resistance to paraquat of this mutant. (H_2O); wild-type n=200, *SOD-CAT-TRX;dPPCS*$^{1/1}$ n=200, *dPPCS*$^{1/1}$ n=173, *dPANK/fbl*$^{1/1}$ n=105, *dPPAT-DPCK*$^{43/43}$ n=102, (H_2O_2); wild-type n=199, *SOD-CAT-TRX;dPPCS*$^{1/1}$ n=101, *dPPCS*$^{1/1}$ n=196, *dPANK/fbl*$^{1/1}$ n=149, *dPPAT-DPCK*$^{43/43}$ n=138, (DTT); wild-type n=190, *SOD-CAT-TRX;dPPCS*$^{1/1}$ n=101, *dPPCS*$^{1/1}$ n=192, *dPANK/fbl*$^{1/1}$ n=170, *dPPAT-DPCK*$^{43/43}$ n=113, (paraquat); wild-type n=191, *SOD-CAT-TRX;dPPCS*$^{1/1}$ n=200, *dPPCS*$^{1/1}$ n=186, *dPANK/fbl*$^{1/1}$ n=116, *dPPAT-DPCK*$^{43/43}$ n=169.
(B) Cysteine survival graph. The percentage of homozygous adults in the F1 generation from crossing heterozygous males and females after feeding larvae a 100 mM L-cysteine solution is plotted as % survival compared to the percentage of homozygous survivors in control crossings (H_2O only). The percentage homozygous survivors under control conditions is set to 100%. *dPANK*$^{1/1}$ and *dPPCS*$^{1/1}$, but not *dPPAT-DPCK*$^{43/43}$ larvae are sensitive to 100 mM L-cysteine. The sensitivity of the *dPPCS*$^{1/1}$ and *dPANK/fbl*$^{1/1}$ mutants could be suppressed by overexpression of ROS scavengers (*SOD-CAT-TRX;dPPCS*$^{1/1}$ and *SOD-CAT-TRX;dPANK/fbl*$^{1/1}$), suggesting that L-cysteine inflicts an oxidative stress response.
(C) Ability to climb in the presence of ROS scavengers. 7-d-old *dPPCS*$^{1/1}$ and *dPPAT-DPCK*$^{43/43}$ males have impaired negative geotaxis as compared to wild-type males. Flies overexpressing ROS scavengers (*SOD-CAT-TRX*) have normal climbing behavior as compared to wild-type flies. Overexpression of SOD-CAT-TRX in a *dPPCS*$^{1/1}$ or in a *dPPAT-DPCK*$^{43/43}$ mutant background did not suppress the *dPPCS*$^{1/1}$ (*SOD-CAT-TRX;dPPCS*$^{1/1}$) and *dPPAT-DPCK*$^{43/43}$ (*SOD-CAT-TRX;dPPAT-DPCK*$^{43/43}$) associated inability to climb against gravity, while, as a positive control, overexpression of *P[dPPCS]* rescued the locomotor defects associated with a mutation in *dPPCS*

triacylglycerol and sterol esters (neutral lipids) during oogenesis was reduced in the CoA mutants (not shown). Moreover, a 2-fold reduction in phosphatidylserine (PS), phosphatidylcholine (PC) and phosphatidylethanolamine (PE) was found in head homogenates from *dPPCS*$^{1/33}$ flies (**Fig. 6B**). This reduction in phospholipids likely reflects a global effect on phospholipid production, since the percentages of PS, PE and PC of the total pool of phospholipids was similar to the percentages found in wild-type heads (**Fig. 6B**). Finally, consistent with a defect in lipid synthesis, the pericerebral fat body was almost absent in 30-d-old *dPPCS*$^{1/33}$ flies compared to wild-type flies of identical age (**Figs. 6C,D**). These data demonstrate that mutations in CoA synthesis affect lipid homeostasis and since lipid metabolism was impaired in all three CoA mutants this strongly suggests that this common feature, downstream of *de novo* CoA synthesis itself, contributes to the neurodegenerative phenotype in the CoA mutants.

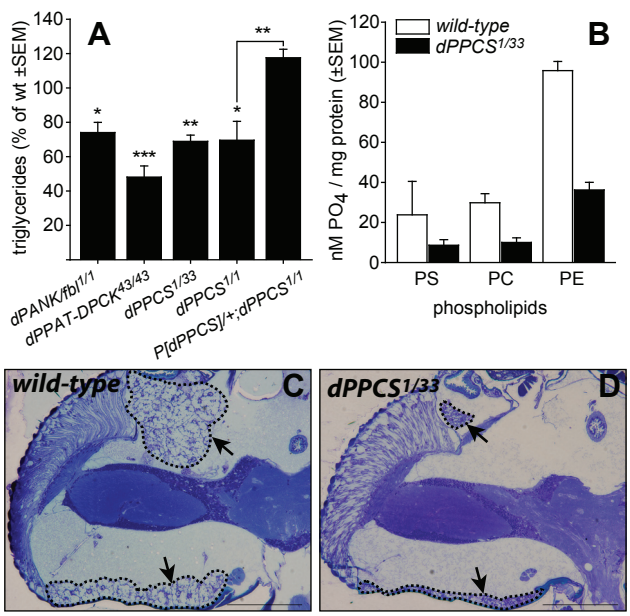

Figure 6. CoA mutant flies display impaired lipid homeostasis.
(A) Triglyceride content of wild-type and mutant flies. The amount of triglycerides was determined in young *dPANK/fbl* (5-d-old) and aged *dPPCS* and *dPPAT-DPCK* mutants (14-d-old), and normalized to levels of wild-type flies of identical age. Adults of all three CoA mutants have approximately 25% less stored fatty acids in the form of triglycerides compared to wild-type flies. (*$p < 0.05$, **$p < 0.005$, ***$p < 0.001$ as determined by *t*-test)
(B) Phospholipids per mg protein were determined in wild-type and *dPPCS*$^{1/33}$ flies. Head homogenates from 14-d-old *dPPCS*$^{1/33}$ flies contain approximately 2-fold less phosphatidylserine (PS), phosphatidylcholine (PC) and phosphatidylethanolamine (PE) compared to wild-type flies. Bars represent the average measured over 2 independent experiments.
(C-D) Horizontal head sections stained with toluidine blue showing the pericerebral fad bodies (arrows) in 30-d-old wild-type (C) and *dPPCS*$^{1/33}$ (D) flies. The pericerebral fat body is almost absent in *dPPCS*$^{1/33}$ flies compared to wild-type flies (dashed lines). 3 flies were investigated for both genotypes and showed the same reduction in pericerebral fat body size. Scale bars; 100 μm

Impaired CoA biosynthesis affects DNA integrity and cellular survival in the developing brain

Since *dPPCS*^{l} was identified as a gene required to survive IR induced DNA damage, we wondered whether and how this is linked to neuronal dysfunction. Like *dPPCS* mutants, *dPANK/fbl* and *dPPAT-DPCK* mutants were also hypersensitive to IR, demonstrating that altered CoA biosynthesis causes DNA damage hypersensitivity (**Fig. 7A**). To identify a possible cause for IR sensitization we first analyzed whether there was a link between oxidative damage and sensitivity to IR in *dPPCS* mutants. However, *SOD-CAT-TRX;dPPCS*$^{1/1}$ mutants displayed hypersensitivity to IR (**Fig. 7A**), indicating that IR sensitization is not due to enhanced levels of oxidative stress.

Previously, it was reported that larval brains of *dPANK/fbl* mutants show increased levels of abnormal mitotic chromosomes[11]. The presence of abnormal mitotic structures is indicative for the presence of higher levels of sustained damaged DNA[36] and we investigated whether impaired CoA biosynthesis in general leads to spontaneous higher levels of DNA damage in proliferating cells and whether this is increased after IR. First, we analyzed mitotic chromosomes in larval brains of the CoA mutants before and 5 h after exposure to 20 Gy (**Fig. 7B**). In non-irradiated mutants a high incidence of abnormal mitotic chromosomes was found, indicating that impaired CoA biosynthesis spontaneously affects DNA integrity. Moreover, the frequency of IR-induced abnormal mitotic structures was higher in all three mutants compared to wild-types (**Fig. 7C**).

Next, we stained the brains with antibodies against phosphorylated Histone 2AvD (γ-H2AvD)[37], a marker for the presence of damaged DNA[38], to test whether aberrant mitoses indeed correlated with higher levels of sustained damaged DNA. Clearly, the brains of *dPANK* and *dPPCS* mutant third instar larvae contained more cells that stained positive for γ-H2AvD than brains from wild-type larvae (**Figs. 7Da-e, Ea**). Although, a small increase in γ-H2AvD positive cells was also observed in *dPPAT-DPCK$^{43/43}$* brains, this increase was not significant. We also investigated whether impaired DNA integrity coincided with increased cell death. Acridine orange uptake in freshly dissected brains revealed that all three CoA mutants displayed enhanced staining compared to wild-type brains, demonstrating that apoptosis was enhanced in mutant larval brains (**Figs. 7Df-g, Eb**). Similarly, increased γ-H2AvD and TUNEL staining was found in *dPPCS$^{1/1}$* follicle cells during early oogenesis, indicating that mutations in CoA synthesis also affects DNA integrity in other proliferating tissues (see **Supplementary Fig. S4**). These data demonstrate that under normal culturing conditions, mutations in CoA biosynthesis result in increased levels of DNA damage in proliferating cells which are further enhanced after exposure to IR, and thus impaired DNA integrity may explain the hypersensitivity to IR.

Finally, to establish a link between IR hypersensitivity and neuronal dysfunction we analyzed the absolute climbing behavior of young (24-h-old) wild-type and *dPPCS$^{1/1}$* flies under control conditions and after IR. In case DNA damage applied to developing larval brains is linked to locomotor dysfunction in young flies, one can predict that IR induces behavioral defects in a wild-type background. For this assay the % of untreated flies that was able to climb was divided by the % of flies that was able to climb after exposure to 20 Gy. Indeed, this ratio for wild-type adults was 1.69 ± 0.13 SEM (n=10), demonstrating that the ability to climb was decreased in young wild-type flies after exposure to IR. Interestingly, in *dPPCS$^{1/1}$* this decreased ability to climb was enhanced compared to wild-types (ratio of untreated to irradiated was 3.23 ± 0.56 SEM, n=10, $p < 0.05$) and was restored in *P[dPPCS]/+;dPPCS$^{1/1}$* flies (1.97 ± 0.15 SEM, n=10, $p < 0.05$). These results suggest an intricate link between impaired DNA integrity and CoA deficiency-associated neuronal dysfunction in young flies.

DISCUSSION

Here we demonstrate that *Drosophila* mutants for *dPANK/fbl*, *dPPCS* and *dPPAT-DPCK* can be used to study the consequences of impaired CoA biosynthesis in higher eukaryotes and our findings strengthen the hypothesis that defective CoA biosynthesis induces a neurodegenerative phenotype[2]. In *Drosophila*, mutations in this conserved pathway lead to increased sensitivity to ROS, impaired DNA integrity in proliferating cells of the developing CNS, cause changes in lipid homeostasis and result in neurologically disturbed flies. Moreover, CoA mutant flies are hypersensitive to IR and because impaired DNA integrity and locomotor dysfunction can be enhanced by IR in CoA mutants and induced in wild-types, our finding suggest that IR hypersensitivity and neuronal dysfunction are at least in part due to impaired DNA integrity.

Our data together with others[2,6,23,32,33] show that there exist similarities and differences between species that carry a mutation in one of the CoA enzymes. All *Drosophila* CoA (including *dPANK/fbl*) mutants display neuronal dysfunction and locomotor defects. PKAN patients that carry a mutation in *PANK2* suffer from motor symptoms such as dystonia or parkinsonism, cognitive decline, and retinal degeneration. These symptoms are often presented during early childhood and progress rapidly (reviewed in ref. 6). In Pank2 deficient mice, no movement abnormalities were observed, however, retinal degeneration was reported[23]. In general, a mutation in human *PANK2* or *Drosophila dPANK/fbl* induces a more severe phenotype as compared to PanK2 depletion in mice. It is possible that in mice (and not in humans) PanK1, PanK3 and/or PanK4 activities can partly compensate for loss of PanK2 function. In addition, differences were reported in expression levels and localization between human PANK2 and mouse PanK2 in brains[26]. Together these differences may explain why PanK2 knock-out mice have a milder neurological phenotype compared to PANK2 deficiency in PKAN patients. Because *Drosophila* has only 1 *PANK/fbl* gene that encodes 4 isoforms, loss of dPANK/Fbl likely causes a more severe phenotype compared to PANK2 deficiency in mammals.

The *Drosophila* CoA mutants display abnormalities in lipid homeostasis, which is consistent with the fact that CoA is required for lipid metabolism[1,25], and impaired lipid metabolism has also been implicated in PKAN disease pathogenesis[2,32,33]. Similarly, hypersensitivity of *dPPCS* and *dPANK/fbl*, but not of *PPAT-DPCK* mutants to cysteine is also consistent with our current knowledge about the conserved biosynthesis pathway of CoA, in which cysteine is incorporated in the second step of this pathway (**Figs. 2A-B**). Increased levels of cysteine have been found in a few patients with clinical symptoms of PKAN[7], suggesting that abnormal cysteine metabolism is present in PKAN patients. Furthermore, patients with PKAN display iron accumulation in specific areas of the brain[6] and together with high levels of cysteine this led to the hypothesis that impaired iron/cysteine metabolism may drive the Fenton reaction[8], leading to the production of ROS[2]. We show that overexpression of ROS scavengers can rescue the sensitivity to cysteine, indicating that lethality induced by cysteine is due to increased levels of oxidative stress. These data, together with the enhanced sensitivity of CoA mutants to ROS, indicate that impaired CoA metabolism leads to enhanced levels of oxidative stress. However, our data also suggest that in addition to oxidative stress, there are other consequences of impaired *de novo* CoA synthesis that may induce neurodegeneration in *Drosophila*. This is based on the observation that overexpression of ROS scavengers did not improve the locomotor defects in young flies. However, it needs to be mentioned that these scavengers are not effective in mitochondria and therefore we can not exclude that in *Drosophila* CoA mutants, neurodegeneration is partly caused by increased oxidative stress within the mitochondria.

Besides abnormal lipid and cysteine metabolism and enhanced levels of oxidative stress, we unexpectedly found that CoA mutant larvae were hypersensitive to IR and their brains displayed increased levels of impaired DNA integrity. Hypersensitivity to IR, enhanced levels of γ-H2AvD, abnormal mitosis, and induction of locomotor dysfunction by IR indicate that locomotor dysfunction in young flies is at least partly due to impaired DNA integrity. We demonstrate that abnormal chromosome organization and increased levels of DNA damage are present in dividing cells of CoA mutants, suggesting that CoA is required for proper cytokinesis. These results are consistent with the observation that cytokinesis was abrogated in the testis of *dPANK/fbl* mutants males[11]. Cytokinesis defects were also found in the *dPPCS* mutant (CHAPTER 6). It may be that changes in lipid homeostasis, especially phospholipids, disrupts the integrity of membranes in the CoA mutants. Depletion of the lipid stores and reduced production of lipids may hamper the renewal of damaged membranes and lipid peroxides, thereby affecting the integrity of tissues including the CNS. Alternatively and not mutually exclusive, aberrant membrane lipid composition might disturb the dynamic interplay between cytoskeletal components, membrane structures and lipid related signaling, leading to division errors during

→ Figure 7. CoA mutant larval brains display abnormal mitosis, show enhanced apoptosis and accumulate DSBs.
(A) IR survival graph. Survival was analyzed as in **Fig. 1A**. *dPANK/fbl*$^{1/1}$ and *dPPAT-DPCK*$^{43/43}$ flies are sensitive to 20 Gy IR. Overexpression of SOD-CAT-TRX did not suppress the hypersensitivity to IR of *dPPCS*$^{1/1}$ mutants (*SOD-CAT-TRX;dPPCS*$^{1/1}$), demonstrating that enhanced oxidative damage is not the primary cause of IR sensitization.
(B) Visualization of mitotic structures. Third instar larval brain mitotic chromosomes from wild-type and mutant larvae 5 h after recovery from 20 Gy IR or left untreated were visualized with antibodies against pH3Ser10 and analyzed for mitotic abnormalities. (Ba-Bc) Normal mitotic chromosomes: metaphase (Ba), anaphase bridge (Bb), anaphase (Bc). (Bd-Bf) Abnormal mitotic chromosomes: fragmented chromosomes (Bd), lagging chromosome (Be), multiple centrosomes (Bf).
(C) Quantification of aberrant mitoses as observed in B. Untreated *dPANK/fbl*$^{1/1}$, *dPPCS*$^{1/33}$ and *dPPAT-DPCK*$^{43/43}$ brains contained a high percentage of abnormal mitosis. The amount of abnormal mitosis increased in all mutants 5 h after recovery from 20 Gy. The number of brains investigated was: (untreated); wild-type n=21, *dPANK/fbl*$^{1/1}$ n=17, *dPPCS*$^{1/1}$ n=17, *dPPCS*$^{1/33}$ n=34, *dPPAT-DPCK*$^{43/43}$ n=14, (20 Gy: 5 h recovery); wild-type n=24, *dPANK/fbl*$^{1/1}$ n=15, *dPPCS*$^{1/1}$ n=21, *dPPCS*$^{1/33}$ n=35, *dPPAT-DPCK*$^{43/43}$ n=12.
(Da-e) Wild-type and mutant third instar larval brains were fixed and labeled with an antibody against γ-H2AvD to detect DSBs and analyzed by confocal laser scanning microscopy (CLMS). (Da,b) Representative images of a wild-type and a mutant third instar larval optic lobe showing enhanced DNA damage (anterior is to the left). Images represent maximal projections of a z-stacks through an entire optic lobe. (Dc-e) High magnification of a field of 3 cells that contain γ-H2AvD foci (arrows). The DNA is visualized with DAPI.
(Df-g) Freshly dissected wild-type and mutant brains were stained with acridine orange and investigated by fluorescent microscopy to detect apoptotic cells. Representative images of a wild-type and a mutant third instar larval optic lobe showing enhanced apoptosis (anterior is to the left).
(E) Quantification of the amount of γ-H2AvD positive cells in brains (Ea) and % of brains showing increased levels of apoptosis (Eb) in wild-types and CoA mutants. Brains were scored as non-apoptotic (Df) or as enhanced apoptotic (Dg). **(Ea)** *dPANK/fbl*$^{1/1}$, *dPPCS*$^{1/1}$ and *dPPCS*$^{1/33}$, but not *dPPAT-DPCK*$^{43/43}$ third instar larval brains contained significantly more cells that stained positive for γ-H2AvD, suggesting that these brains accumulate elevated levels of DSBs. Ectopic expression of 1 copy of the *P[dPPCS]* transgene reduced the amount of γ-H2AvD positive cells in *dPPCS*$^{1/1}$ (*P[dPPCS]/+;dPPCS*$^{1/1}$), but 2 copies were required to reduce the amount of γ-H2AvD positive cells back to wild-type levels (*P[dPPCS];dPPCS*$^{1/1}$). The amount of brains investigated was: wild-type n=25, *dPANK/fbl*$^{1/1}$ n=25, *dPPAT-DPCK*$^{43/43}$ n=12, *dPPCS*$^{1/33}$ n=17, *dPPCS*$^{1/1}$ n=23, *P[dPPCS]/+;dPPCS*$^{1/1}$ n=19 and *P[dPPCS];dPPCS*$^{1/1}$ n=16. **(Eb)** Compared with wild-type brains, the brains of *dPANK/fbl*$^{1/1}$, *dPPCS*$^{1/33}$, *dPPCS*$^{1/1}$ and *dPPAT-DPCK*$^{43/43}$ larvae display enhanced acridine orange staining, which indicates that cells within these brains are apoptotic (percentages are depicted at the top of each histogram). The amount of brains investigated was: wild-type n=20, *dPANK/fbl*$^{1/1}$ n=20, *dPPAT-DPCK*$^{43/43}$ n=21, *dPPCS*$^{1/33}$ n=20, *dPPCS*$^{1/1}$ n=21, *P[dPPCS]/+;dPPCS*$^{1/1}$ n=20, and *P[dPPCS];dPPCS*$^{1/1}$ n=20. (*$p < 0.05$, **$p < 0.005$, ***$p < 0.001$ as determined by *t*-test). Scale bars; 50 μm (Da,b,f,g), 6 μm (Dc-e)

CNS development that in turn may result in impaired DNA integrity. Therefore it is possible that abnormal lipid homeostasis directly leads to impaired neuronal function and this neuronal dysfunction is enhanced by increased DNA damage as a result of these lipid abnormalities. Several neurological disorders are associated with defects in DNA repair[39], but increased DNA damage has never been linked to altered CoA biosynthesis, to PKAN or to PanK2 depletion in mice.

Although currently we can not explain all the inter-species differences, the presented *Drosophila* model, in addition to the mouse model, may be of help to unravel the complex pathology of PKAN and to understand the importance of CoA for CNS development and function.

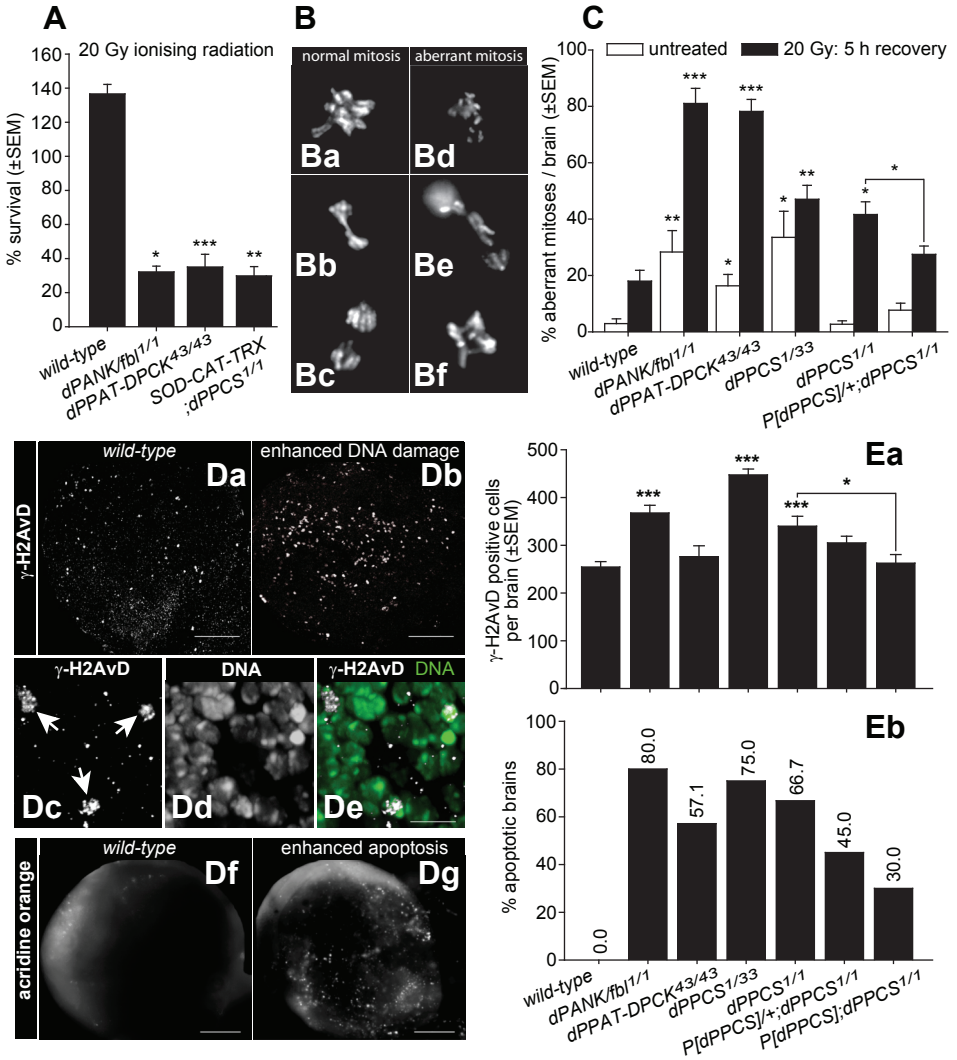

ACKNOWLEDGEMENTS

We thank R. S. Sohal for providing the *ZnSod-Cat-Trx* fly line; J. Sekelsky for the pBUF plasmid; L. G. Fradkin for the pCaSpeR4-Pme1-Bgh plasmid; J. Hageman, E. B. van Lacum, M. A. Rujano, E. Seinen and J. M. van der Wouden for technical advice and assistance; P. Rump and G. de Haan for critical reading of this manuscript and valuable comments. This work was supported by a VIDI grant from the Netherlands Organization for Scientific Research (NWO; 971-36-400) to O. C. M. S. and by an UMCG Topmaster Grant to A. R.

LITERATURE CITED

1. Leonardi, R., Zhang, Y. M., Rock, C. O. & Jackowski, S. Coenzyme A: back in action. *Prog. Lipid Res.* **44**, 125-153 (2005).
2. Zhou, B. *et al.* A novel pantothenate kinase gene (PANK2) is defective in Hallervorden-Spatz syndrome. *Nat. Genet.* **28**, 345-349 (2001).
3. Begley, T. P., Kinsland, C. & Strauss, E. The biosynthesis of coenzyme A in bacteria. *Vitam. Horm.* **61**, 157-171 (2001).
4. Daugherty, M. *et al.* Complete reconstitution of the human coenzyme A biosynthetic pathway via comparative genomics. *J. Biol. Chem.* **277**, 21431-21439 (2002).
5. Kupke, T., Hernandez-Acosta, P. & Culianez-Macia, F. A. 4'-phosphopantetheine and coenzyme A biosynthesis in plants. *J. Biol. Chem.* **278**, 38229-38237 (2003).
6. Hayflick, S. J. Unraveling the Hallervorden-Spatz syndrome: pantothenate kinase-associated neurodegeneration is the name. *Curr. Opin. Pediatr.* **15**, 572-577 (2003).
7. Perry, T. L. *et al.* Hallervorden-Spatz disease: cysteine accumulation and cysteine dioxygenase deficiency in the globus pallidus. *Ann. Neurol.* **18**, 482-489 (1985).
8. Imlay, J. A., Chin, S. M. & Linn, S. Toxic DNA damage by hydrogen peroxide through the Fenton reaction in vivo and in vitro. *Science* **240**, 640-642 (1988).
9. Galvin, J. E., Giasson, B., Hurtig, H. I., Lee, V. M. & Trojanowski, J. Q. Neurodegeneration with brain iron accumulation, type 1 is characterized by alpha-, beta-, and gamma-synuclein neuropathology. *Am. J. Pathol.* **157**, 361-368 (2000).
10. Ke, Y. & Ming Qian, Z. Iron misregulation in the brain: a primary cause of neurodegenerative disorders. *Lancet Neurol.* **2**, 246-253 (2003).
11. Afshar, K., Gonczy, P., DiNardo, S. & Wasserman, S. A. fumble encodes a pantothenate kinase homolog required for proper mitosis and meiosis in Drosophila melanogaster. *Genetics* **157**, 1267-1276 (2001).
12. Orr, W. C., Mockett, R. J., Benes, J. J. & Sohal, R. S. Effects of overexpression of copper-zinc and manganese superoxide dismutases, catalase, and thioredoxin reductase genes on longevity in Drosophila melanogaster. *J. Biol. Chem.* **278**, 26418-26422 (2003).
13. Robertson, H. M. *et al.* A stable genomic source of P element transposase in Drosophila melanogaster. *Genetics* **118**, 461-470 (1988).
14. Cooley, L., Kelley, R. & Spradling, A. Insertional mutagenesis of the Drosophila genome with single P elements. *Science* **239**, 1121-1128 (1988).
15. Guo, Y. *et al.* Site-selected mutagenesis of the Drosophila second chromosome via plasmid rescue of lethal P-element insertions. *Genome Res.* **6**, 972-979 (1996).
16. Muhlig-Versen, M. *et al.* Loss of Swiss cheese/neuropathy target esterase activity causes disruption of phosphatidylcholine homeostasis and neuronal and glial death in adult Drosophila. *J. Neurosci.* **25**, 2865-2873 (2005).
17. Benzer, S. Genetic dissection of behavior. *Sci. Am.* **229**, 24-37 (1973).
18. Palladino, M. J., Hadley, T. J. & Ganetzky, B. Temperature-sensitive paralytic mutants are enriched for those causing neurodegeneration in Drosophila. *Genetics* **161**, 1197-1208 (2002).
19. Strauss, E., Kinsland, C., Ge, Y., McLafferty, F. W. & Begley, T. P. Phosphopantothenoylcysteine synthetase from Escherichia coli. Identification and characterization of the last unidentified coenzyme A biosynthetic enzyme in bacteria. *J. Biol. Chem.* **276**, 13513-13516 (2001).
20. Genschel, U. Coenzyme A biosynthesis: reconstruction of the pathway in archaea and an evolutionary scenario based on comparative genomics. *Mol. Biol. Evol.* **21**, 1242-1251 (2004).
21. Kotzbauer, P. T., Truax, A. C., Trojanowski, J. Q. & Lee, V. M. Altered neuronal mitochondrial coenzyme A synthesis in neurodegeneration with brain iron accumulation caused by abnormal processing, stability, and catalytic activity of mutant pantothenate kinase 2. *J. Neurosci.* **25**, 689-698 (2005).
22. Hortnagel, K., Prokisch, H. & Meitinger, T. An isoform of hPANK2, deficient in pantothenate kinase-associated neurodegeneration, localizes to mitochondria. *Hum. Mol. Genet.* **12**, 321-327 (2003).
23. Kuo, Y. M. *et al.* Deficiency of pantothenate kinase 2 (Pank2) in mice leads to retinal degeneration and azoospermia. *Hum. Mol. Genet.* **14**, 49-57 (2005).
24. Leonardi, R., Rock, C. O., Jackowski, S. & Zhang, Y. M. Activation of human mitochondrial pantothenate kinase 2 by palmitoylcarnitine. *Proc. Natl. Acad. Sci. U. S. A* **104**, 1494-1499 (2007).
25. Zhang, Y. M. *et al.* Chemical knockout of pantothenate kinase reveals the metabolic and genetic program responsible for hepatic coenzyme A homeostasis. *Chem. Biol.* **14**, 291-302 (2007).
26. Leonardi, R., Zhang, Y. M., Lykidis, A., Rock, C. O. & Jackowski, S. Localization and regulation of mouse pantothenate kinase 2. *FEBS Lett.* **581**, 4639-4644 (2007).
27. Kuo, Y. M., Hayflick, S. J. & Gitschier, J. Deprivation of pantothenic acid elicits a movement disorder and

azoospermia in a mouse model of pantothenate kinase-associated neurodegeneration. *J. Inherit. Metab Dis.* (2007).
28. Abiko, Y., Ashida, S. I. & Shimizu, M. Purification and properties of D-pantothenate kinase from rat liver. *Biochim. Biophys. Acta* **268**, 364-372 (1972).
29. Lin, M. T. & Beal, M. F. Mitochondrial dysfunction and oxidative stress in neurodegenerative diseases. *Nature* **443**, 787-795 (2006).
30. Kretzschmar, D. Neurodegenerative mutants in Drosophila: a means to identify genes and mechanisms involved in human diseases? *Invert. Neurosci.* **5**, 97-109 (2005).
31. Dodson, M. W. & Guo, M. Pink1, Parkin, DJ-1 and mitochondrial dysfunction in Parkinson's disease. *Curr. Opin. Neurobiol.* **17**, 331-337 (2007).
32. Houlden, H. *et al.* Compound heterozygous PANK2 mutations confirm HARP and Hallervorden-Spatz syndromes are allelic. *Neurology* **61**, 1423-1426 (2003).
33. Danek, A. & Walker, R. H. Neuroacanthocytosis. *Curr. Opin. Neurol.* **18**, 386-392 (2005).
34. Min, K. T. & Benzer, S. Preventing neurodegeneration in the Drosophila mutant bubblegum. *Science* **284**, 1985-1988 (1999).
35. Tschape, J. A. *et al.* The neurodegeneration mutant lochrig interferes with cholesterol homeostasis and Appl processing. *EMBO J.* **21**, 6367-6376 (2002).
36. Gorski, M. M. *et al.* Disruption of Drosophila Rad50 causes pupal lethality, the accumulation of DNA double-strand breaks and the induction of apoptosis in third instar larvae. *DNA Repair (Amst)* **3**, 603-615 (2004).
37. Redon, C. *et al.* Histone H2A variants H2AX and H2AZ. *Curr. Opin. Genet. Dev.* **12**, 162-169 (2002).
38. Rogakou, E. P., Boon, C., Redon, C. & Bonner, W. M. Megabase chromatin domains involved in DNA double-strand breaks in vivo. *J. Cell Biol.* **146**, 905-916 (1999).
39. Barzilai, A. The Contribution of the DNA Damage Response to Neuronal Viability. *Antioxid. Redox. Signal.* (2007).